DOI: 10.1002/chem.200801255

Self-Assembly of Oligo(*para*-phenylenevinylene)s through Arene—Perfluoroarene Interactions: π Gels with Longitudinally Controlled Fiber Growth and Supramolecular Exciplex-Mediated Enhanced Emission

Sukumaran S. Babu, Vakayil K. Praveen, Seelam Prasanthkumar, and Ayyappanpillai Ajayaghosh*[a]

Abstract: The arene–perfluoroarene (Ar_H–Ar_F) interaction, which has been extensively studied in the field of solid-state chemistry, is exploited in the hierarchical self-assembly of oligo(*para*-phenylenevinylene)s (OPVs) with controlled longitudinal fiber growth that leads to gelation. The size of the self-assembled fibers of a pentafluorophenyl-functionalized OPV **5** could be controlled through C-F···H–C hydrogen bonding and π stacking. The ability of fluoroaromatic compounds to form excited-state complexes with aromatic amines has been utilized to form a supramolecular exciplex, exclusively in the gel state, that exhibits enhanced emission. Thus, the commonly encountered fluorescence quenching during the self-assembly of OPVs could be considerably prevented by exciplex formation with *N*,*N*-dimethylaniline (DMA), which only occurred for the fluorinated OPV and not for the non-fluorinated analogue **4**. In the former case, a threefold enhancement in the emission intensity could be observed in the gel state, whereas no change in emission occurred in solution. Thus, the major limitations of spontaneous fiber growth and fluorescence self-quenching encountered in the self-assembly of OPVs could be controlled to a great extent by using the versatile Ar_H–Ar_F interaction.

Keywords: exciplex · fluorine · organogel · pi-stacking · self-assembly

Introduction

Two important issues that need to be addressed during the bottom-up self-assembly of fluorescent π systems are the controlled growth of the resultant hierarchical architectures and the self-quenching of the fluorescence during the self-assembly. Control of these two processes is essential for applications related to organic electronic devices. As a result of the high propensity toward π stacking, longitudinal control of the self-assembly of linear π-conjugated molecules to supramolecular architectures with controlled aspect ratio and high fluorescence quantum yield is a challenging task.[1] Earlier studies have shown that oligo(*para*-phenylenevinylene)s (OPVs) when functionalized with weak hydrogen-bonding groups spontaneously self-assemble to form supramolecular tapes several micrometers in length, thus leading to the gelation of hydrocarbon solvents.[2] As a result, the fluorescence is shifted to a long wavelength with a significant decrease in the quantum yield. As a result of fast excitation energy migration, energy transfer to a suitable acceptor is possible in these systems, thus leading to tunable emissions with improved quantum yields.[3] However, for a wider application of OPV self-assemblies, it is necessary to control the morphology and the photophysical properties. Therefore, strategies to control the longitudinal propagation of OPV self-assemblies without much decrease in the fluorescence emission are of great significance.

Perfluoroarenes are well-known synthons in crystal engineering.[4–7] Grubbs and co-workers extensively used the arene–perfluoroarene (Ar_H–Ar_F) interaction in favor of [2+2] photocycloaddition, liquid crystal design, and hydrogel formation.[8] Moreover, this strategy is considered to be an effective approach to prepare n-type molecular semiconductors from p-type materials without altering the parent carbon skeleton.[9] Despite its proven utility in the solid state, the Ar_H–Ar_F interaction has not been widely exploited

[a] S. S. Babu, Dr. V. K. Praveen, S. Prasanthkumar, Dr. A. Ajayaghosh
Photosciences and Photonics Group
Chemical Sciences and Technology Division
National Institute for Interdisciplinary Science and Technology (NIIST)
CSIR, Trivandrum-695 019 (India)
Fax: (+91) 471-249-1712
E-mail: ajayaghosh62@gmail.com

Supporting information for this article is available on the WWW under http://dx.doi.org/10.1002/chem.200801255.

in the self-assembly of molecular architectures in solution.[8a,10] This is mainly as a result of the weak nature of the Ar_H–Ar_F interaction in solution.[4] Recently, Feast and co-workers reported that 4,4′-bis(2,3,4,5,6-pentafluorostyryl)stilbene self-assembles through Ar_H–Ar_F interactions, thus leading to a brickwall-type arrangement of molecules in the crystal packing.[7] We took advantage of this property to control the spontaneous, lengthwise self-assembly of π-conjugated systems with a controlled aspect ratio of the resulting fibers, thus leading to the gelation of organic solvents.[2,11]

In addition to the above reasons, we thought of taking advantage of the proven ability of fluorinated π-conjugated molecules to form exciplexes with electron-donating aromatic amines. Bazan and co-workers have carried out extensive studies on exciplex formation between fluorinated distyrylbenzene derivatives and *N*,*N*-dimethylaniline (DMA).[5c,e] Exciplexes of π-conjugated molecules are known to have strong emissions.[12–15] However, this strategy has not been utilized to improve the emission of supramolecular architectures and organogels, although a few reports are available on the enhanced induced emission of aggregates.[16] Herein, we report for the first time the ability of the Ar_H–Ar_F interaction to control the aspect ratio of self-assembled architectures of linear π-systems with enhanced emission through a supramolecular exciplex formation exclusively in the gel state.

Results and Discussion

Synthesis: The OPV derivatives **4** and **5** were synthesized as outlined in Scheme 1 and were characterized by NMR spectroscopy, IR spectroscopy, and MALDI-TOF mass spectrometry. The pentafluorophenyl-functionalized OPV **5** was prepared from the OPV bis-aldehyde **1** by the reaction of the corresponding phosphonate ester **3** in THF in presence of NaH in 86% yield.[2g,17] For a comparative study, the OPV derivative **4** without the fluorine atoms was prepared in 85% yield (Scheme 1).

Optical properties: Details of the photophysical parameters of OPV derivatives **4** and **5** in THF and *n*-decane at a concentration of 1×10^{-5} M are given in Table 1. The absorption and emission maxima, fluorescence quantum yields, and lifetimes of **4** and **5** were significantly different in these solvents. For example, **5** exhibits a high fluorescence quantum yield and a longer lifetime than **4** in THF. The absorption spectra of **4** and **5** in THF (1×10^{-5} M) exhibited maxima of around $\lambda_{max}=442$ and 447 nm, respectively, whereas in *n*-decane (1×10^{-4} M) they showed broad absorption with a red-shifted shoulder at around $\lambda=520$ nm, thus indicating molecular aggregation (Figure 1).[2] In *n*-decane at 20 °C, the absorption spectrum of **5** showed a shoulder band at $\lambda=523$ nm in addition to the π–π* transition band ($\lambda_{max}=428$ nm). As the temperature is increased to 65 °C, the shoulder band disappeared with an increase in the intensity of the π–π* transition band. Under these conditions, the absorption spectrum matches that in THF, except a small blue-shift in the absorption maximum ($\lambda_{max}=506$ nm).

The emission spectra of **4** and **5** in THF were broad with an emission maximum of around $\lambda_{max}=520$ nm. In *n*-decane (1×10^{-4} M) at 20 °C, the emission maximum at $\lambda_{max}=520$ nm

Table 1. Optical parameters of OPV derivatives **4** and **5** in THF and *n*-decane.[a]

Compd	Solvent	λ_{abs} [nm]	λ_{em} [nm]	log ε	Φ_f	τ [ns]
	THF	442	520, 553	5.75	0.54	1.13
4	*n*-decane	427	536, 575	4.50	0.09	1.71 (61%)
						0.74 (39%)
	THF	447	511, 540	5.73	0.70	1.28
5	*n*-decane	428	541, 582	4.57	0.11	1.88 (68%)
						0.83 (32%)

[a] Fluorescence quantum yields (±5% error) were determined using 10-methylacridinium triflouromethanesulfonate as the standard ($\Phi_r=0.99$ in water).[18] All the measurements were carried out at a concentration of 1×10^{-5} M, except the fluorescence quantum yield measurement in which the absorbance at the excitation wavelength ($\lambda_{ex}=415$ nm) was adjusted at 0.1.

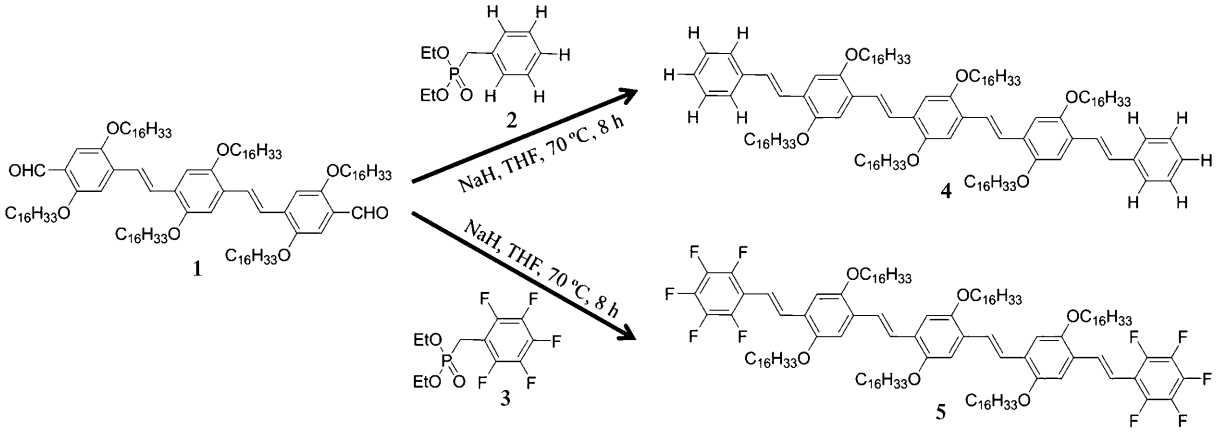

Scheme 1. Synthesis of OPV derivatives **4** and **5**.

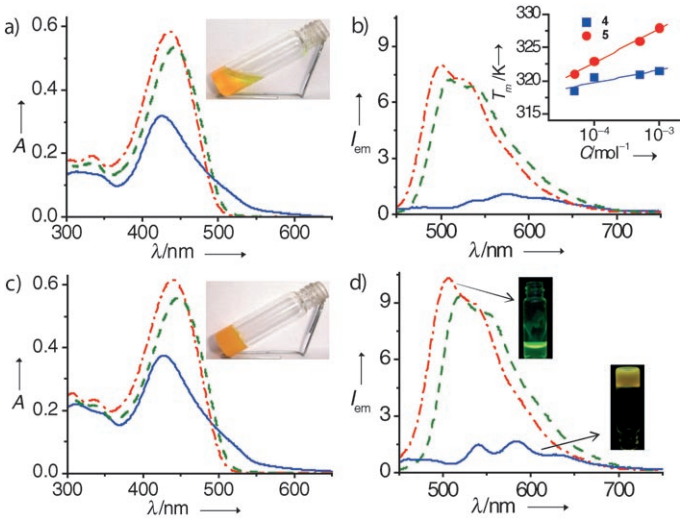

Figure 1. Absorption (a and c) and emission (b and d) of **4** and **5**, respectively, in THF (1×10^{-5} M) and *n*-decane (1×10^{-4} M; $\lambda_{ex}=415$ nm). (– – –) THF at 20 °C, (——) *n*-decane at 20 °C, and (–•–•–) *n*-decane at 65 °C. Insets: a) photograph of nongeling aggregates of **4**, b) plot of the melting temperature T_m of **4** and **5** versus concentration, c) photograph of a gel of **5** in *n*-decane (0.72 mmol), and d) photographs of a gel of **5** at 20 °C and a sol at 65 °C under illumination with 365-nm light. A = absorption, I_{em} = emission intensity, C = concentration.

exhibited strong quenching with a slight redshift, thus indicating aggregation of the molecules. In addition, for **4** the emission was broad in *n*-decane, whereas **5** exhibited a structured emission with three bands at $\lambda=540$, 582, and 635 nm, thereby indicating a better organization of the molecular self-assembly in the latter. However, the emission spectrum at 65 °C resembled those in THF as a result of breaking of the aggregates. Molecules **4** and **5** and their aggregates in *n*-decane (1×10^{-4} M) are photochemically stable, which is essential for any potential application of these molecules. This stability is clear from the absorption and emission spectra, which did not change even after irradiation at $\lambda=365$ nm for 48 h (see the Supporting Information).[19]

Aggregation and gelation properties: Even though **4** and **5** form aggregates in *n*-decane, significant differences in the aggregate stability of these two molecules could be observed, thus indicating the crucial role of the pentafluorophenyl group. For example, comparison of the plots of the melting temperature T_m of the aggregates at different concentration revealed a marked increase in the stability of the aggregates of **5** (Figure 1b, Inset).

Compound **5** showed a sharp increase in the value of T_m with increasing concentration compared with **4**. In addition, significant differences were observed in the spectral features of **4** and **5**, as indicated by the sigmoidal plots of the fraction of aggregates versus temperature (see the Supporting Information). These observations could be attributed to a relatively strong and organized self-assembly of **5** because of the possible arene–perfluoroarene (Ar_H–Ar_F) interaction and additional C–F···H–C hydrogen-bonding interaction, which strengthens the π stacking. This argument is supported by the fact that **5** forms a stable organogel from hydrocarbon solvents, whereas **4** failed to form gels. The remarkable variation in the gelation abilities of **4** and **5** points toward the importance of the Ar_H–Ar_F interaction in the fluorinated OPV, which allows the extended self-assembly of these aggregates to form fibers. The critical gelator concentrations (CGCs) of **5** in *n*-decane, cyclohexane, and toluene at 20 °C are 0.72, 0.76, and 0.97 mmol, respectively, thus indicating that in these solvents **5** behaves as a super gelator (see the Supporting Information).[11c] Plots of the gel melting temperatures T_{gel} versus concentration in *n*-decane, cyclohexane, and toluene revealed that **5** is a better gelator of *n*-decane (see the Supporting Information). The viscoelastic nature of the gels was confirmed by rheological studies by using frequency sweep experiments that indicated that the elastic modulus G' and the viscous modulus G'' values are independent of the oscillation frequency range of 0.01–10 rads^{-1} at a strain of 5% (Torque value $=1.2\times10^2$ μNm). Complex viscosity showed a linear decrease with increasing frequency, thus indicating that the unbroken matrices of the gel show good tolerance to external forces and are mechanically strong. The G' value is nearly an order of magnitude higher than G'', thereby indicating that the gel is elastically stronger and dominates over the viscous properties. When the gelator concentration was increased, the G' value, which is considered to be the measure of resistance to elastic deformation or "stiffness", also increased, thus revealing a gradual increase in the viscoelastic solidlike behavior of the gels (see the Supporting Information).

Morphological studies: Transmission electron microscopy (TEM) studies of a dilute solution of **5** in *n*-decane, drop-cast onto a carbon-coated grid showed the formation of short fibrous structures 1—3 μm in length and approximately 10–100 nm in width, which form bundles of fibers (see Figure 2a). Interestingly, as the concentration was increased from 2.5×10^{-5}–5×10^{-5} M, the length of the fibers gradually increased without much change in the width (Figure 2b). It must be noted that at these concentrations, the length of the fibers formed are significantly shorter than the fibers formed by the previously reported OPV gels, in which spontaneous self-assembly was observed that lead to supramolecular tapes several micrometers in length.[2] A further increase in concentration to 7.5×10^{-5} M showed elongated fibers with an increase in the fiber length with widths of approximately 10–100 nm (Figure 2c). The observed concentration-dependent control of the fiber growth of **5** is remarkable when compared with the spontaneous supramolecular-tape formation of hydrogen-bond-assisted self-assemblies of linear π systems, as reported earlier.[2g,f] Interestingly, TEM analysis of **4** from *n*-decane (5×10^{-5} M) showed the formation of clustered short aggregates. These aggregates failed to form extended fibers on increasing concentration (Figure 2d).

Polarizing optical microscopy (POM) studies of a gel of **5** in *n*-decane (0.72 mmol) exhibited birefringent fibrous ag-

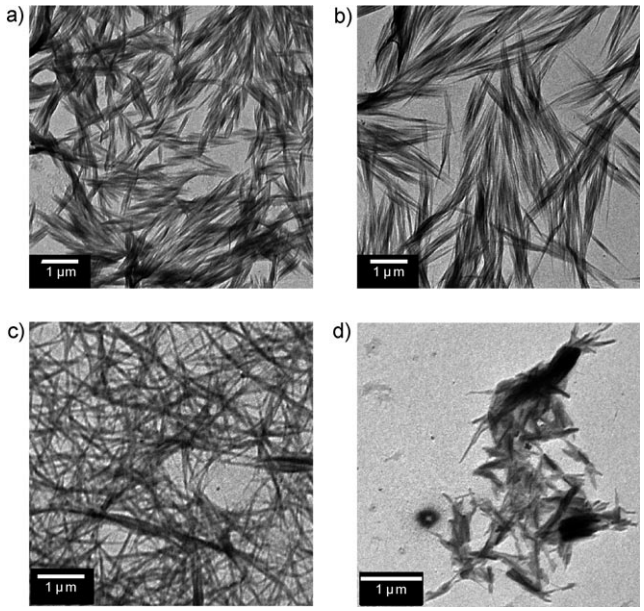

Figure 2. TEM images (unstained) of **5** at different concentrations a) 2.5×10^{-5}, b) 5×10^{-5}, and c) 7.5×10^{-5} M and d) a TEM image of **4** (5×10^{-5} M) in *n*-decane.

gregates on cooling from the isotropic solution, whereas no defined morphology was observed for **4**, thus revealing the anisotropic organization of the molecules in the former case (see the Supporting Information). Possible molecular packing of **5** in the gel state could be achieved from previous reports that pertain to the crystal packing in fluorinated OPVs.[7] In analogy to these reports, it is believed that the electrostatic potential of the opposite sign assists the aggregation of molecules into a brick-wall-type arrangement in which each molecule overlaps with nearly two halves of the neighboring molecules in the row below and above and vice versa (Figure 3a).[7] This behavior is supported by the electron-density distribution in **5**, which showed an inverse electrostatic potential with a partial positive charge at the inner portion of the fluorinated ring (Figure 3b).[4a] It has already been reported that the free energy of formation of benzene and the hexafluorobenzene dimer is negative, and introduction of one fluorine atom to a phenyl ring decreases the stacking repulsion between the phenyl rings by approximately 2 kJ mol^{-1}.[20]

In addition to the favorable Ar_H–Ar_F stacking interactions, intermolecular C–F···H–C interactions may further support the brick-wall-type arrangement.[4,7] Such a controlled organization of **5** will lead to an extended lamellar-type assembly in solution, thus resulting in the formation of fibers that lead to the gelation of solvents. Evidence for the proposed packing mode could be obtained from X-ray diffraction (XRD) patterns of a xerogel of **5** in *n*-decane (Figure 3c). The diffraction signal observed at 3.69 Å in the wide-angle region matches well with the reported value for benzene–hexafluorobenzene co-crystals.[4a,6c,21] A diffraction peak with *d*-spacing of 28.23 Å corresponds to the side-wise packing of the alkyl side chains of the OPVs in the same plane. The *d*-spacings of 9.3, 6.9, and 4.3 Å may correspond to the packing of the alkyl side chains in the brick-wall-type assembly of the OPVs.[2g]

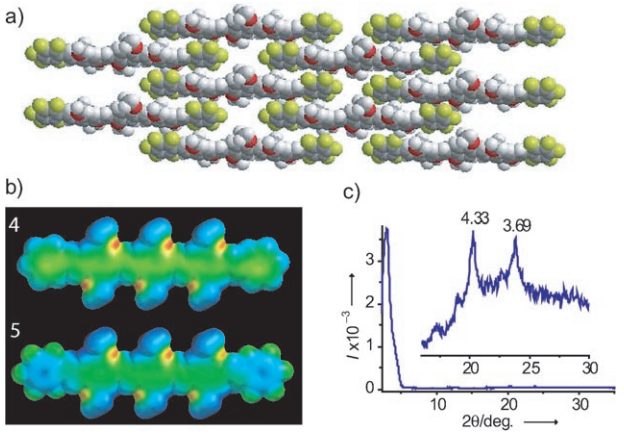

Figure 3. a) A probable molecular-packing diagram of **5** in the gel state. b) Electron-density distributions of **4** and **5** calculated with TITAN software (Wavefunction, Inc). In the computation experiments, the hexadecyloxy side chains in the OPV structure were replaced with methoxy groups. c) XRD pattern of a xerogel of **5** in *n*-decane; inset: a zoomed region between 15–30°.

Effect of DMA in the gelation and optical properties of 5: Surprisingly, **5** was found to gelate pure DMA (2.65 mmol) and DMA/*n*-decane mixtures (Figure 4a). These gels were

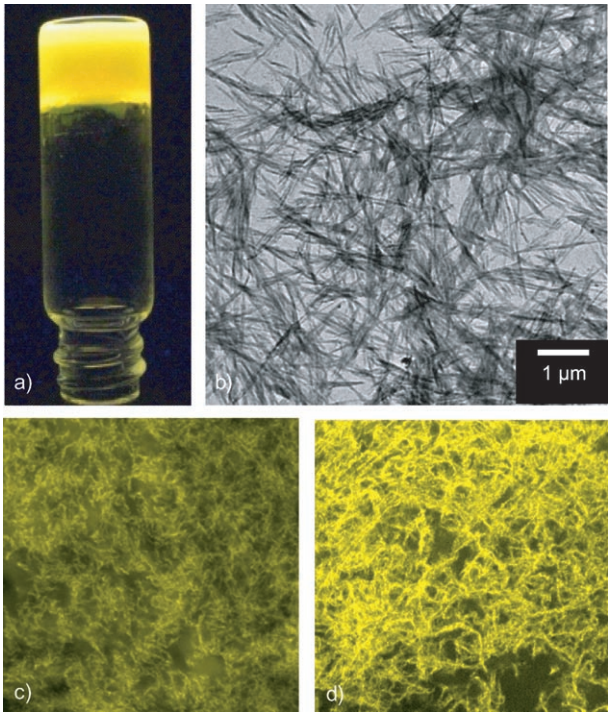

Figure 4. a) Photograph of the **5**+DMA gel in *n*-decane on illumination with 365-nm light at 20°C. b) TEM image (unstained) of **5** (5×10^{-5} M) in the presence of DMA (0.5 M) in *n*-decane. c, d) Confocal laser scanning microscopy images (40×) of the gels of **5** in the absence and presence of DMA, respectively, in *n*-decane ([**5**] = 0.72 mmol, [DMA] = 7.2 mmol, λ_{ex} = 453 nm, λ_{em} = 520–580 nm).

fairly stable, even though a slight decrease in the stability was observed in the presence of DMA when compared to pure *n*-decane gels (see the Supporting Information). A plot of T_{gel} against the weight % of DMA for a *n*-decane gel of **5** showed a decrease with a difference of 5 °C in pure DMA. This observation indicated the intercalation of DMA in between the self-assembly of **5** in the gel state. TEM analysis of **5** in *n*-decane (5×10^{-5} M) containing different amounts of DMA (0.5 M) revealed the formation of short, bundled fibrous assemblies a few micrometers in length and 10–100 nm in width (Figure 4b). Although the size of the fibers decreased in presence of DMA, the overall morphology remained more or less the same. Interestingly, the addition of DMA to the *n*-decane gel of **5** resulted in a considerable increase in the emission intensity when compared to that of the *n*-decane gel. This behavior is clear from a comparison of the fluorescence of the confocal laser scanning microscopy (CLSM) images (Figure 4c,d) of the gels of **5** before and after the addition of DMA.

The remarkable increase in fluorescence upon the addition of DMA could be ascribed either to breaking of the self-assembly or to exciplex formation between **5** and DMA in the gel state. The former possibility is ruled out because **5** forms gels in the presence of DMA. Moreover, TEM and confocal analysis confirmed the presence of fibers, thus indicating the self-assembly of **5** in the presence of DMA. Hence, the reason for the enhanced emission could be the result of exciplex formation between **5** and DMA. Moreover, DMA is chosen as the donor solvent because its role in exciplex formation is well known.[12] The intercalation of DMA in the brick-wall-type assembly of **5** in *n*-decane in the gel state allows proximity between the two moieties, which facilitates supramolecular exciplex formation when the latter is excited (see the Supporting Information).[22] In agreement with Jenekhe and Osaheni, it is reasonable to expect excimer formation in such an assembly because the OPV **5** is already organized into a potential excimer-forming configuration in the supramolecular assembly.[13]

For better insight into the phenomenon, quantitative studies were performed by adding different amounts of DMA to a gel of **5** (8.3×10^{-5} M) in *n*-decane, and a gradual increase in the emission intensity when excited at $\lambda=415$ nm was seen (Figure 5a). Upon the addition of 0.83 M DMA, the intensity of the weak structured emission of the gel increased with broadening. The possibility of breaking of the self-assembly for the observed fluorescence enhancement is ruled out because the absorption spectrum of the gel did not vary much upon the addition of DMA (Figure 5, inset). This observation also reveals that there is no ground-state charge-transfer interaction between **5** and DMA, which was also established from the comparison of the excitation spectra of **5** and **5**+DMA monitored at $\lambda=565$ nm at 20 °C in *n*-decane (see the Supporting Information). In both cases, the excitation spectra exhibited the broad absorption of the self-assembled OPVs. Therefore, as stated previously, the likely cause of the increase in emission intensity could be attributed to exciplex formation. This argument is supported by the

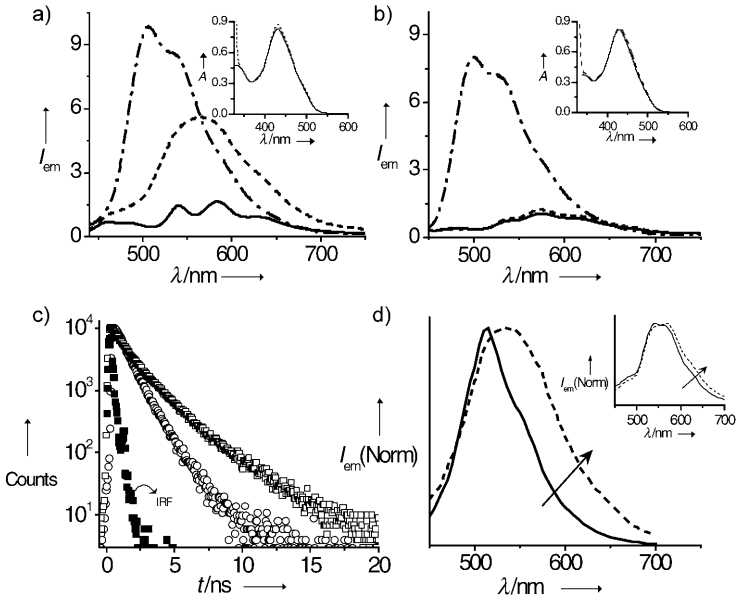

Figure 5. Emission spectra of a) **5** (8.3×10^{-5} M) and b) **4** (8.3×10^{-5} M) in *n*-decane at 20 °C (——), in *n*-decane at 65 °C (–•–•), and in *n*-decane + 0.83 M DMA at 20 °C (– – –) ($\lambda_{ex}=415$ nm); inset: the corresponding changes in the absorption spectra. c) Fluorescence decay profiles of **5** in the monomeric state (○) and in the gel state in presence of DMA (□) in *n*-decane monitored at $\lambda=565$ nm ($\lambda_{ex}=440$ nm). IRF = instrument response function. d) TRES of **5** in the presence of 0.83 M DMA at 56 ps (——) and 1.7 ns (– – –) after excitation at $\lambda=440$ nm at 20 °C in *n*-decane (8.3×10^{-5} M); inset: the TRES of **5** in the absence of DMA in *n*-decane at 56 ps (——) and 1.1 ns (– – –) after excitation at $\lambda=440$ nm at 20 °C.

report by Wang and Bazan on exciplex formation between DMA and distyrylbenzene derivatives.[5c] Because the monomer emission was already shifted toward a longer wavelength as a result of gelation, a further shift in the emission was not observed for the supramolecular exciplex. However, when compared to the monomer emission, the exciplex showed a 50-nm redshift. The absolute quantum yields of **5** in the gel form (10.83 %) showed a maximum threefold enhancement to 31.29 % upon the addition of DMA.[23] The fluorescence decay profiles of **5** showed a monoexponential decay of 1.28 ns in the monomeric state (Figure 5c). The exciplex of **5** with DMA in the gel state exhibited a biexponential decay with lifetimes of 0.82 and 3.26 ns (31 and 69 %, respectively). As the temperature was increased, the broad emission became more intense with a blue shift, thus indicating breaking of the exciplex to the corresponding monomers (see the Supporting Information).

The time-resolved emission spectrum (TRES) of **5** obtained at 56 ps after the excitation at $\lambda=440$ nm exhibited a broad emission that did not show any major shift with time (Figure 5d, inset). However, the TRES of **5** in the presence of DMA exhibited a relatively narrow emission at 56 ps with a maximum around $\lambda=500$ nm (Figure 5d). After a time delay of 1.7 ns, a broad emission at $\lambda=550$ nm was obtained. It is important to note that the time delay required for such a dynamic shift in the emission of **5** in the absence

of DMA is approximately 1.1 ns, which indicates fast excited-state decay dynamics. In the presence of DMA, this process is delayed, which indicates the formation of an excited complex between the intercalated DMA and **5**.

Interestingly, the addition of DMA to the aggregates of **4** showed only a marginal increase in the emission, thus indicating a weak interaction between the two in the excited state (Figure 5b). It is also clear that DMA could not break up the aggregates into monomers, in which case the emission intensity should have increased. Therefore, it is obvious that the perfluoroarene moieties play an important role in exciplex formation. Moreover, it must be noted that exciplex formation between **5** and DMA occurs only in the gel state. In the solution state, the addition of DMA did not result in any significant change in the emission spectrum or fluorescence quantum yield of **5** (see the Supporting Information). This observation in the solution state is analogous to a report by Wang and Bazan and is ascribed to the effect of conjugation length on exciplex formation.[5c] An increase in the conjugation length of the acceptor may cause a drop in the excited-state singlet energy more quickly than the electron affinity and hence exciplex formation is not favored. However, this limitation could be overcome in the case of **5** in the gel state. Thus, the Ar_H–Ar_F interaction plays an important role in the gelation of OPVs and in modulating the photophysical behavior through supramolecular exciplex formation.

Conclusion

In conclusion, we have unraveled the role of the Ar_H–Ar_F interaction in the controlled growth of self-assembled architectures of linearly π-conjugated molecules on the nanometer-to-micrometer scale. This strategy has been demonstrated for the first time in the hierarchical self-assembly of OPVs in solution with controlled fiber size, which is otherwise difficult to achieve. Moreover, the usually encountered quenching of fluorescence emission of OPV gels could be prevented to a great extent through exciplex formation. This example of a π gel that forms supramolecular exciplexes exclusively in the gel state with enhanced emission and controlled size of the self-assembled architectures is unique. Thus, the arene–perfluoroarene interaction has been demonstrated not only to induce self-assembly of OPVs in solution, thus leading to gelation, but also to be efficient in preventing the uncontrolled propagation and decreased fluorescence quantum yields of the self-assembly. These results broaden the application of arene–perfluoroarene interactions in the area of supramolecular chemistry.

Experimental Section

General methods: Unless otherwise stated, all the starting materials and reagents were purchased from commercial suppliers and used without further purification. The solvents were purified and dried by standard methods prior to use. Melting points were determined with a Mel-Temp-II melting point apparatus and are uncorrected. ^{1}H and ^{13}C NMR spectra were measured on a 300 MHz Bruker Avance DPX spectrometer using trimethylsilane (TMS) as an internal standard. Fourier-transform infrared (FTIR) spectra were recorded on a Shimadzu IRPrestige-21 FTIR spectrophotometer. Matrix-assisted laser desorption ionization time-of-flight (MALDI-TOF) mass spectra were obtained on a Perseptive Biosystems Voyager DE-Pro MALDI-TOF mass spectrometer with α-cyano-4-hydroxycinnamic acid as the matrix. The starting bisaldehyde **1** was prepared as reported previously.[2g]

Preparation of 4 and 5: NaH (3.7 mmol) was added carefully to a solution of phosphonate ester **2** or **3** (1.12 mmol) and bis-formyl derivative **1** (0.56 mmol) in THF (35 mL) under argon. The reaction mixture was stirred at 70 °C for 8 h, and the solvent was removed under reduced pressure. The resultant residue was extracted with chloroform and washed several times with saturated brine and water. The organic layer was dried over anhydrous Na_2SO_4 and concentrated to give the corresponding products. Further purification was carried out by column chromatography (hexane/chloroform, 3:1) on silica gel (100—200 mesh).

4: Yield: 85%; m.p. 105–107 °C; ^{1}H NMR (300 MHz, $CDCl_3$, TMS): δ = 0.85–0.87 (t, 18H, CH_3), 1.24–1.87 (m, 168H, CH_2), 4.04–4.06 (m, 12H, OCH_2), 7.11–7.16 (m, 8H, Ar-H), 7.34–7.38 (t, 6H, Ar-H), 7.46–7.55 ppm (m, 10H, Ar-H); ^{13}C NMR ($CDCl_3$, 75 MHz): δ = 14.11, 22.69, 26.26, 26.34, 26.37, 28.30, 29.10, 29.37, 29.57, 29.73, 31.93, 69.19, 110.11, 110.54, 112.92, 114.08, 123.29, 126.49, 128.62, 135.38, 136.72, 138.35, 145.9 ppm; FTIR (KBr): $\tilde{\nu}_{max}$ = 692, 722, 750, 803, 849, 964, 1018, 1071, 1099, 1207, 1259, 1348, 1350, 1388, 1423, 1465, 1506, 1596, 2849, 2921 cm^{-1}; MALDI-TOF MS: *m/z*: calcd for 1929.19: found: 1929.27.

5: Yield: 86%; m.p. 114–116 °C; ^{1}H NMR (300 MHz, $CDCl_3$, TMS): δ = 0.85–0.87 (t, 18H, CH_3), 1.24–1.86 (m, 168H, CH_2), 4.05 (t, 12H, OCH_2), 7.07–7.16 (m, 8H, Ar-H), 7.64–7.5 (m, 4H, Ar-H), 7.7–7.76 ppm (d, 2H, Ar-H); ^{13}C NMR ($CDCl_3$, 75 MHz): δ = 14.11, 22.71, 25.9, 26.32, 26.41, 28.33, 29.10, 29.36, 29.6, 29.75, 31.93, 69.10, 110.64, 111.01, 114.92, 116.08, 125.6, 126.51, 127.4, 128.62, 135.32, 137.71, 138.35, 145.93 ppm; FTIR (KBr): $\tilde{\nu}_{max}$ = 695, 721, 750, 801, 853, 1023, 1097, 1204, 1261, 1350, 1385, 1423, 1465, 1500, 1629, 2849, 2921, 2956 cm^{-1}; MALDI-TOF MS: *m/z*: calcd for 2107.61; found: 2107.22.

Optical measurements: Electronic absorption spectra were recorded on a Shimadzu UV-3101 PC NIR scanning spectrophotometer and the emission spectra were recorded on a SPEX-Flourolog F112X spectrofluorimeter. Temperature-dependent studies were carried out with a thermistor directly attached to the wall of the cuvette holder. Fluorescence quantum yields Φ_s of OPVs in THF are reported relative to 10-methylacridinium triflouromethanesulfonate (Φ_r = 0.99 in water). The experiments were done using optically matching solutions and the quantum yield is calculated by using Equation (1):[18]

$$\Phi_s = \Phi_r(A_r F_{s/} A_s F_r)(\eta_s^2/\eta_r^2) \quad (1)$$

where A_s and A_r are the absorbance of the sample and reference solutions, respectively, at the same excitation wavelength; F_s and F_r are the corresponding relative integrated fluorescence intensities, respectively; and η is the refractive index of the solvents used.

Fluorescence quantum yield in the gel state: The fluorescence quantum yield of gels was measured using a calibrated integrating sphere in an SPEX Fluorolog spectrofluorimeter. A Xe arc lamp was used to excite the sample placed in the sphere with λ = 415 nm as the excitation wavelength.

The absolute fluorescence quantum yield was calculated based on the de Mello method[23] by using Equation (2):

$$\Phi_{PL} = [E_i(\lambda) - (1-A)E_0(\lambda)]/L_e(\lambda)A \quad (2)$$

For Equation (2):

$$A = [L_o(\lambda) - L_i(\lambda)]/L_o(\lambda) \quad (3)$$

where $E_i(\lambda)$ and $E_0(\lambda)$ are the integrated luminescence as a result of the

direct excitation of sample and secondary excitation, respectively; A is the absorbance of the sample calculated using Equation (3); $L_i(\lambda)$ is the integrated excitation when the sample is directly excited; $L_0(\lambda)$ is the integrated excitation when the excitation light first hits the sphere and reflects into the sample; and $L_e(\lambda)$ is the integrated excitation profile for an empty sphere.

The fluorescence lifetimes and time-resolved emission spectra (TRES) were measured by using the IBH (FluoroCube) time-correlated picosecond single-photon counting (TCSPC) system. Details of the instrumental set up are given in the Supporting Information.

Morphological studies: TEM was performed on a FEI, TEC NAI 30 G2 S-TWIN microscope with an accelerating voltage of 100 kV. Samples were prepared by drop-casting solutions of OPV in *n*-decane onto carbon-coated copper grids, and the TEM pictures were obtained without staining.

CLSM images were recorded on a Leica-DMIR2 optical microscope using UV light ($\lambda = 453$ nm) as the excitation source and the emission was collected between $\lambda = 520$ and 580 nm with 40× magnification. The samples were prepared by drop-casting a solution in *n*-decane onto a glass slide followed by slow evaporation.

The samples for the XRD studies were prepared by transferring a hot solution of OPV in *n*-decane onto a glass slide, which was allowed to cool and dry slowly. The X-ray diffractograms of the dried films were recorded on a Phillips diffractometer by using Ni-filtered $Cu_{K\alpha}$ radiation.

Exciplex emission studies: Samples for exciplex emission studies were prepared by transferring the required amount of the solutions of **4** or **5** in *n*-decane and DMA from the stock solution to a 1-mm cuvette. During these studies, the concentrations of **4**, **5**, and DMA were kept constant at 8.3×10^{-5} and 0.83 M, respectively. After thorough mixing, the solution was heated to 50 °C and allowed to cool to room temperature. In the case of **5**, bright fluorescent gels were obtained. Samples for the solution-state studies were also prepared in the same way by thorough mixing without heating and cooling.

Detailed descriptions and the experimental data of the gelation, gel melting, spectroscopy, microscopy, and rheology studies are given in the Supporting Information.

Acknowledgements

We thank the Department of Science and Technology (DST; New Delhi, India) for financial support under the Nano Science and Technology Initiative and the CSIR network programme (NWP0023). A.A. acknowledges DST for a Ramanna Fellowship. S.S.B., V.K.P., and S.P. are grateful to the Council of Scientific and Industrial Research (CSIR) for fellowships. We acknowledge Mr. P. Gurusamy, Mr. R. Philip, and Dr. J.D. Sudha of NIIST and Dr. R.V. Omkumar of the Rajiv Gandhi Centre for Biotechnology (RGCB) for the XRD, TEM, rheology, and confocal laser scanning microscopy studies, respectively. This is contribution No. PPG-272.

[1] a) F. J. M. Hoeben, P. Jonkheijm, E. W. Meijer, A. P. H. J. Schenning, *Chem. Rev.* **2005**, *105*, 1491–1546; b) for a review of supramolecular dye chemistry, see: C.-C. You, R. Dobrawa, C. R. Saha-Möller, F. Würthner, *Top. Curr. Chem.* **2005**, *258*, 39–82; c) A. Ajayaghosh, S. J. George, A. P. H. J. Schenning, *Top. Curr. Chem.* **2005**, *258*, 83–118.

[2] a) A. Ajayaghosh, V. K. Praveen, *Acc. Chem. Res.* **2007**, *40*, 644–656; b) A. Ajayaghosh, V. K. Praveen, S. Srinivasan, R. Varghese, *Adv. Mater.* **2007**, *19*, 411–415; c) J. van Herrikhuyzen, S. J. George, M. R. J. Vos, N. A. J. M. Sommerdijk, A. Ajayaghosh, S. C. J. Meskers, A. P. H. J. Schenning, *Angew. Chem.* **2007**, *119*, 1857–1860; *Angew. Chem. Int. Ed.* **2007**, *46*, 1825–1828; d) A. Ajayaghosh, C. Vijayakumar, R. Varghese, S. J. George, *Angew. Chem.* **2006**, *118*, 470–474; *Angew. Chem. Int. Ed.* **2006**, *45*, 456–460; e) V. K. Praveen, S. J. George, A. Ajayaghosh, *Macromol. Symp.* **2006**, *241*, 1–8; f) R. Varghese, S. J. George, A. Ajayaghosh, *Chem. Commun.* **2005**, 593–595; g) S. J. George, A. Ajayaghosh, *Chem. Eur. J.* **2005**, *11*, 3217–3227; h) A. Ajayaghosh, S. J. George, *J. Am. Chem. Soc.* **2001**, *123*, 5148–5149.

[3] a) A. Ajayaghosh, V. K. Praveen, C. Vijayakumar, *Chem. Soc. Rev.* **2008**, *37*, 109–122; b) A. Ajayaghosh, V. K. Praveen, C. Vijayakumar, S. J. George, *Angew. Chem.* **2007**, *119*, 6376–6381; *Angew. Chem. Int. Ed.* **2007**, *46*, 6260–6265; c) V. K. Praveen, S. J. George, R. Varghese, C. Vijayakumar, A. Ajayaghosh, *J. Am. Chem. Soc.* **2006**, *128*, 7542–7550; d) A. Ajayaghosh, C. Vijayakumar, V. K. Praveen, S. S. Babu, R. Varghese, *J. Am. Chem. Soc.* **2006**, *128*, 7174–7175; e) A. Ajayaghosh, S. J. George, V. K. Praveen, *Angew. Chem.* **2003**, *115*, 346–349; *Angew. Chem. Int. Ed.* **2003**, *42*, 332–335.

[4] a) K. Reichenbächer, H. I. Süss, J. Hulliger, *Chem. Soc. Rev.* **2005**, *34*, 22–30; b) M. Pagliaro, R. J. Ciriminna, *J. Mater. Chem.* **2005**, *15*, 4981–4991; c) S. Lorenzo, G. R. Lewis, I. Dance, *New J. Chem.* **2000**, *24*, 295–304; d) C. R. Patrick, G. S. Prosser, *Nature* **1960**, *187*, 1021–1021.

[5] a) Z. Wang, F. Dötz, V. Enkelmann, K. Müllen, *Angew. Chem.* **2005**, *117*, 1273–1276; *Angew. Chem. Int. Ed.* **2005**, *44*, 1247–1250; b) F. Ponzini, R. Zagha, K. Hardcastle, J. S. Siegel, *Angew. Chem.* **2000**, *112*, 2413–2415; *Angew. Chem. Int. Ed.* **2000**, *39*, 2323–2325; c) S. Wang, G. C. Bazan, *Chem. Phys. Lett.* **2001**, *333*, 437–443; d) G. P. Bartholomew, X. Bu, G. C. Bazan, *Chem. Mater.* **2000**, *12*, 2311–2318; e) M. L Renak, G. P. Bartholomew, S. Wang, P. J. Ricatto, R. J. Lachicotte, G. C. Bazan, *J. Am. Chem. Soc.* **1999**, *121*, 7787–7799; f) B. Strehmel, A. M. Sarker, J. H. Malpert, V. Strehmel, H. Seifert, D. C. Neckers, *J. Am. Chem. Soc.* **1999**, *121*, 1226–1236.

[6] a) S. W. Watt, C. Dai, A. J. Scott, J. M. Burke, R. L. Thomas, J. C. Collings, C. Viney, W. Clegg, T. B. Marder, *Angew. Chem.* **2004**, *116*, 3123–3125; *Angew. Chem. Int. Ed.* **2004**, *43*, 3061–3063; b) C. E. Smith, P. S. Smith, R. L. Thomas, E. G. Robins, J. C. Collings, C. Dai, A. J. Scott, S. Borwick, A. S. Batsanov, S. W. Watt, S. J. Clark, C. Viney, J. A. K. Howard, W. Clegg, T. B. Marder, *J. Mater. Chem.* **2004**, *14*, 413–420; c) C. Dai, P. Nguyen, T. B. Marder, A. J. Scott, W. Clegg, C. Viney, *Chem. Commun.* **1999**, 2493–2494.

[7] a) R. Capelli, M. A. Loi, C. Taliani, H. B. Hansen, M. Murgia, G. Ruani, M. Muccini, P. W. Lovenich, W. J. Feast, *Synth. Met.* **2003**, *139*, 909–912; b) W. J. Feast, P. W. Lövenich, H. Puschmann, C. Taliani, *Chem. Commun.* **2001**, 505–506.

[8] a) A. F. M. Kilbinger, R. H. Grubbs, *Angew. Chem.* **2002**, *114*, 1633–1636; *Angew. Chem. Int. Ed.* **2002**, *41*, 1563–1566; b) M. Weck, A. R. Dunn, K. Matsumoto, G. W. Coates, E. B. Lobkovsky, R. H. Grubbs, *Angew. Chem.* **1999**, *111*, 2909–2912; *Angew. Chem. Int. Ed.* **1999**, *38*, 2741–2745; c) G. W. Coates, A. R. Dunn, L. M. Henling, J. W. Ziller, E. B. Lobkovsky, R. H. Grubbs, *J. Am. Chem. Soc.* **1998**, *120*, 3641–3649; d) G. W. Coates, A. R. Dunn, L. M. Henling, D. A. Dougherty, R. H. Grubbs, *Angew. Chem.* **1997**, *109*, 290–293; *Angew. Chem. Int. Ed. Engl.* **1997**, *36*, 248–251.

[9] F. Babudri, G. M. Farinola, F. Naso, R. Ragni, *Chem. Commun.* **2007**, 1003–1022.

[10] a) A. Hori, A. Akasaka, K. Biradha, S. Sakamoto, K. Yamaguchi, M. Fujita, *Angew. Chem.* **2002**, *114*, 3403–3406; *Angew. Chem. Int. Ed.* **2002**, *41*, 3269–3272; b) M. J. Marsella, Z.-Q. Wang, R. J. Reid, K. Yoon, *Org. Lett.* **2001**, *3*, 885–887.

[11] a) *Molecular Gels, Materials with Self-Assembled Fibrillar Networks* (Eds.: P. Terech, R. G. Weiss), Kluwer Press, Dordrecht, The Netherlands, **2005**; b) T. Ishi-i, S. Shinkai, *Top. Curr. Chem.* **2005**, *258*, 119–160; c) R Luboradzki, O. Gronwald, A. Ikeda, S. Shinkai, *Chem. Lett.* **2000**, 1148; d) J. H. van Esch, B. L. Feringa, *Angew. Chem.* **2000**, *112*, 2351–2354; *Angew. Chem. Int. Ed.* **2000**, *39*, 2263–2266.

[12] a) N. J. Turro, *Modern Molecular Photochemistry*, Benjamin-Cummings, Menlo Park, California, **1978**, p. 135; b) A. Weller in *The Exciplex* (Eds.: M. Gordon, W. Ware), Academic Press, New York, **1975**, pp. 23–28.

[13] a) S. A. Jenekhe, *Adv. Mater.* **1995**, *7*, 309–311; b) S. A. Jenekhe, J. A. Osaheni, *Science* **1994**, *265*, 765–768; c) J. A. Osaheni, S. A. Je-

nekhe, *Macromolecules* **1994**, *27*, 739–742; d) J. A. Osaheni, S. A. Jenekhe, *Macromolecules* **1993**, *26*, 4126–4128.

[14] a) J. Kalinowski, M. Cocchi, D. Virgili, V. Fattori, J. A. G. Williams, *Adv. Mater.* **2007**, *19*, 4000–4007; b) C. Yin, T. Kietzke, D. Neher, H.-H. Hörhold, *Appl. Phys. Lett.* **2007**, *90*, 092117; c) A. C. Morteani, A. S. Dhoot, J. S. Kim, C. Silva, N. C. Greenham, C. Murphy, E. Moons, S. Cina, R. H. Friend, *Adv. Mater.* **2003**, *15*, 1708–1712; d) H. Meier, *Angew. Chem.* **2001**, *113*, 1903–190; *Angew. Chem. Int. Ed.* **2001**, *40*, 1851–1853; e) J.-F. Wang, Y. Kawabe, S. E. Shaheen, M. M. Morrell, G. E. Jabbour, P. A. Lee, J. Anderson, N. R. Armstrong, B. Kippelen, E. A. Mash, N. Peyghambarian, *Adv. Mater.* **1998**, *10*, 230–233.

[15] a) D. W. Cho, M. Fujitsuka, K. H. Choi, M. J. Park, U. C. Yoon, T. Majima, *J. Phys. Chem. B* **2006**, *110*, 4576–4582; b) T. Offermans, P. A. van Hal, S. C. J. Meskers, M. M. Koetse, R. A. J. Janssen, *Phys. Rev. B* **2005**, *72*, 045213, 1–11.

[16] a) X. Yang, R. Lu, T. Xu, P. Xue, X. Liu Y. Zhao, *Chem. Commun.* **2008**, 453–455; b) P. Xue, R. Lu, G. Chen, Y. Zhang, H. Nomoto, M. Takafuji, H. Ihara, *Chem. Eur. J.* **2007**, *13*, 8231- 8239; c) N. S. S. Kumar, S. Varghese, G. Narayan, S. Das, *Angew. Chem.* **2006**, *118* 6465–6469; *Angew. Chem. Int. Ed.* **2006**, *45*, 6317–6321; d) J. F. Hulvat, M. Sofos, K. Tajima, S. I. Stupp, *J. Am. Chem. Soc.* **2005**, *127*, 366–372; e) B.-K. An, D.-S. Lee, J.-S. Lee, Y.-S. Park, H.-S. Song, S. Y. Park, *J. Am. Chem. Soc.* **2004**, *126*, 10232–10233; f) S. Y. Ryu, S. Kim, J. Seo, Y.-W. Kim, O.-H. Kwon, D.-J. Jang, S. Y. Park, *Chem. Commun.* **2004**, 70–71; g) H. Iharaa, T. Yamadaa, M. Nishiharaa, T. Sakuraia, M. Takafujia, H. Hachisakob, T. Sagawa, *J. Mol. Liq.* **2004**, *111*, 73–76; h) B.-K. An, S.-K. Kwon, S.-D. Jung, S. Y. Park, *J. Am. Chem. Soc.* **2002**, *124*, 14410–14415; i) R. Deans, J. Kim, M. R. Machacek, T. M. Swager, *J. Am. Chem. Soc.* **2000**, *122*, 8565–8566.

[17] B. Wang, M. R. Wasielewski, *J. Am. Chem. Soc.* **1997**, *119*, 12–21.

[18] a) J. R. Lakowicz, *Principles of Fluorescence Spectroscopy*, 2nd ed., Kluwer Academic/Plenum Publishers, New York, **1999**; b) G. Weber, F. W. J. Teale, *Trans. Faraday Soc.* **1957**, *53*, 646–655; c) S. A. Jonker, F. Ariese, J. W. Verhoeven, *Recl. Trav. Chim. Pays-Bas.* **1989**, *108*, 109–115.

[19] Y. Kim, T. M. Swager, *Chem. Commun.* **2005**, 372–374.

[20] a) R. Laatikainen, J. Ratilainen, R. Sebastian, H. Santa, *J. Am. Chem. Soc.* **1995**, *117*, 11006–11010; b) F. Cozzi, F. Ponzini, R. Annunziata, M. Cinquini, J. S. Siegel, *Angew. Chem.* **1995**, *107*, 1092–1094; *Angew. Chem. Int. Ed. Engl.* **1995**, *34*, 1019–1021; c) R. Laatikainen, H. Santa, Y. Hiltunen, J. Lounila, *J. Magn. Reson.* **1993**, *A104*, 238–241.

[21] D. G. Naae, *Acta Crystallogr. Sect. B: Struct. Sci.* **1979**, *35*, 2765–2768.

[22] a) R. Huenerbein, S. Grimme, *Chem. Phys.* **2008**, *343*, 362–371; b) R. Ide, Y. Shikata, S. Misumi, T. Ikada, N. Mataga, *J. Chem. Soc. Chem. Commun.* **1972**, 1009.

[23] a) L.-O. Pålsson, A. P. Monkman, *Adv. Mater.* **2002**, *14*, 757–758; b) J. C. de Mello, H. F. Wittmann, R. H. Friend, *Adv. Mater.* **1997**, *9*, 230–232.

Received: June 24, 2008
Published online: September 9, 2008

